

Loading tests of bored piles inserted nodular and cylindrical piles

S.Kanai

Takechi Engineering Co., Ltd, Tokyo, Japan

S.Yabuuchi

Takechi Engineering Co., Ltd, Osaka, Japan

ABSTRACT: This report describes the results of comparison loading tests on the bearing capacity of cylindrical and nodular piles. Load tests of piles in the vertical and horizontal in direction were carried out at two locations using cylindrical piles with a smooth surface and nodular piles with nodes at 1m intervals, which were set with cement milk injection method. Reinforcing bar stress transducer were attached to each test pile to measure the applied load and bending moment. The results of both tests show that the nodular pile had more favorable bearing capacity. The nodular pile also had a larger ultimate bearing capacity than the cylindrical pile, showing that skin friction acting on the piles worked effectively. With regard to the horizontal bearing capacity, although the bending rigidity was different by about two times in both pile types, the horizontal resistance were almost equal.

1 INTRODUCTION

In Japan, foundation methods with which noise and vibration are reduced are adopted when carrying out pile foundation work of buildings in urban areas in order to minimize the effect of that on the neighboring residents and buildings. As a foundation method when using pre-cast concrete piles, the cement milk injection

method shown in Fig. 1 is most frequently used. In this method, ground is excavated using an auger screw to drill a hole in the ground.

After the auger screw is pulled out while injecting fluid such as cement milk into the drilled hole from the tip of the auger screw, a reinforced concrete pile is inserted into the drilled hole, and the pile top is lightly driven by a drop hammer, etc.

The test was made to compare the difference in the vertical and horizontal bearing capacity between a cylindrical pile having a smooth surface like that of a round reinforcing bar and a nodular pile like that of a deformed reinforcing bar. The test was carried out at two locations: one in Fukuoka prefecture (CASE 1) and the other in Osaka (CASE 2).

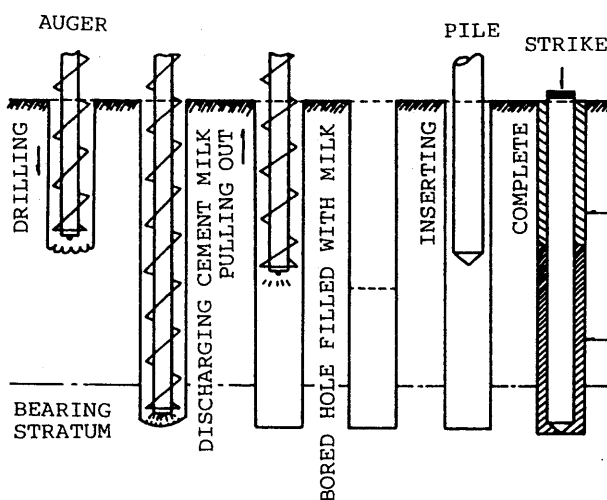


Fig.1 Cement Milk Injection Method

2 SOIL CONDITION AND TEST PROCEDURE

As shown in Fig. 2, the soil condition in CASE 1 was alternated between with layers of silt and sand. The tips of the test piles penetrated 2.4 m in the sand layer which was 7.60 m depth from the ground surface. Meanwhile, the soil condition in CASE 2 consisted of sand and gravel layers interlocked with layers of silt and clay. The tips of the piles penetrated 3.60 m

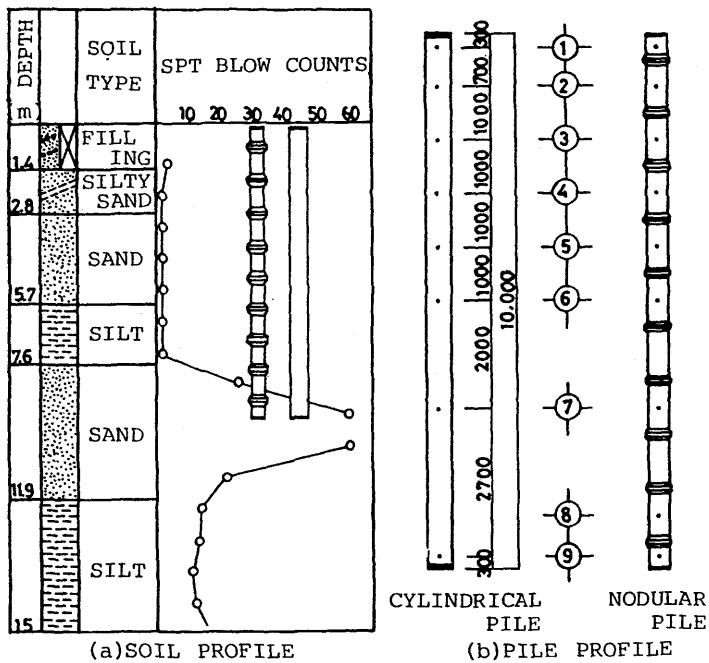


Fig.2 Soil and Pile Profile (CASE 1)

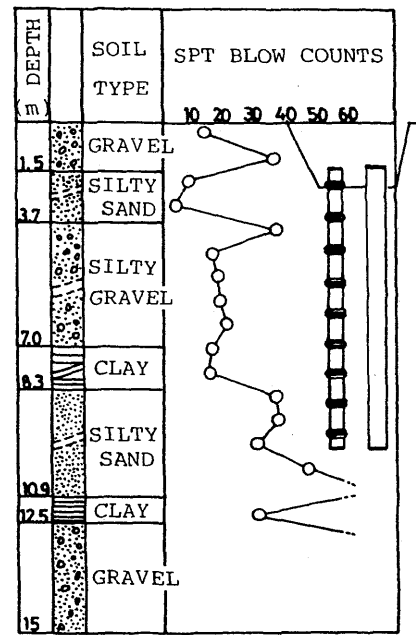


Fig.3 Soil Profile (CASE 2)

in the silty sand layer which was 8.35 m depth from the ground level. Nodular piles of 500 mm diameter were used. Both piles were made of high strength prestressed concrete. The pile length was 10 m in CASE 1 and 9 m in CASE 2. Table 1 shows the specifications of the piles. In CASE 1, a reinforcing bar stress transducers was attached to measure the axial load of the pile during a vertical load test as shown in Fig. 2. In CASE 2, a 20 cm steel pipe having the same outer diameter as that of that of the piles was connected to the pile so that a strain gauge could be fitted on the pipe.

Table.1 Size and stiffness

CASE	Diameter (mm)	Knob D. (mm)	Thickness (mm)	Stiffness ($10^4 \cdot \text{KNm}^2$)
1	400	500	65	4.01
	500	-	90	10.25
2	400	500	65	4.10
	500	-	70	9.68

In the vertical load test, the maximum planned load decided to assume the ultimate bearing capacity of the pile based on the soil boring log shown in Figs. 2 and 3. The maximum load was divided into more than

eight steps, and load was applied by setting the loading speed constant so that load were maintained uniformly for each load level at any time. In CASE 1, both the dead load of some concrete blocks and the tension force generated by pulling out anchor piles were used as a reaction device for applying load while in CASE 2, only the pulling resistance of the anchor piles was used as a reaction device.

In the horizontal load test, repeat load was applied in three cycles by applying force into one direction in Case 1 whereas in CASE 2, loading devices were placed on both sides of the test pile and repeat load was alternately applied in 4-5 cycles by operating the devices.

During the vertical load test, repeat load and settlement at the pile head, strain on the pile shaft, and settlement of the pile end were measured whereas in the horizontal load test, load, displacement at force adding position and strain of the pile shaft were measured.

3 TEST RESULTS

3.1 Results of Vertical Load Test

The relationship between load and settlement on the pile head is shown in Fig.4 and Fig.5. Axial load acting on the pile shaft was calculated based on the records obtain-

ed from the reinforcing bar stress transducer and the strain gauge, and the distribution of axial load by depth is shown in Fig.6 and Fig.7. As is clear from Fig.4 and 5, in both cases, the nodular piles showed better load-settlement characteristics compared with cylindrical piles. In both cases, since the piles did not reach the ultimate load, the ultimate load was assumed by the Van Der Veen method. Results are shown in Table 2.

Fig.6 and 7 show that both the cylindrical and nodular piles have a similar axial load distribution during the load applied on the pile head is small, but that the end axial

load of the cylindrical piles increased at an earlier loading stage than that of the nodular piles. Fig.8 was prepared to investigate the process of load transmission from the pile head to the pile end.

Table 2 Ultimate Bearing Capacity

CASE	Nodular Pile KN	Cylindrical Pile KN
1	3,430	2,352
2	4,410	3,822

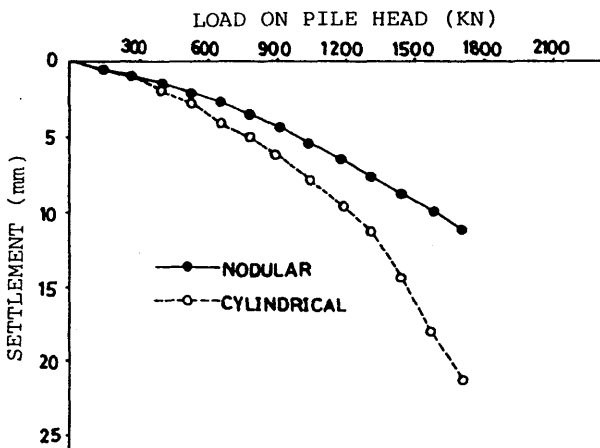


Fig.4 Relationship between Load and Settlement (CASE.1)

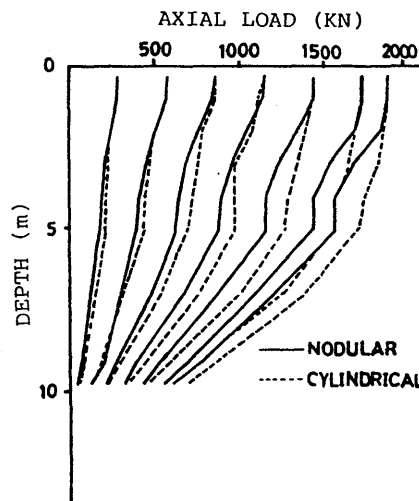


Fig.6 Distribution of Axial Load (CASE.1)

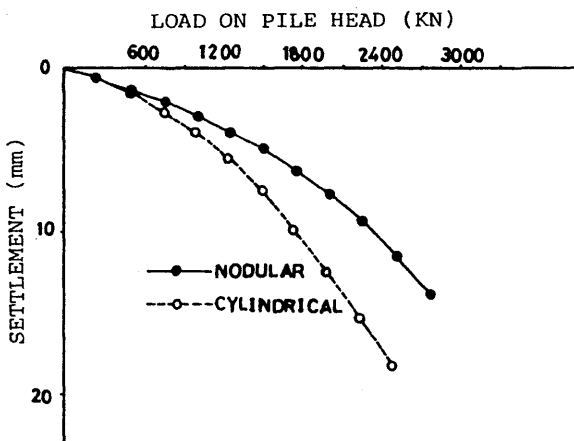


Fig.5 Relationship between Load and Settlement (CASE.2)

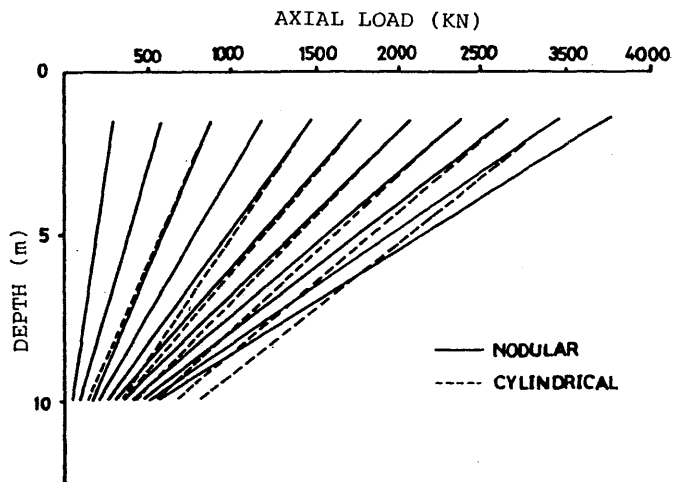


Fig.7 Distribution of Axial Load (CASE.2)

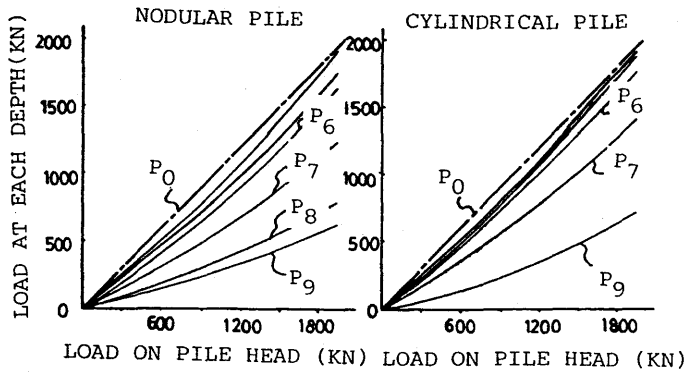


Fig.8 Load transmission (CASE.1)

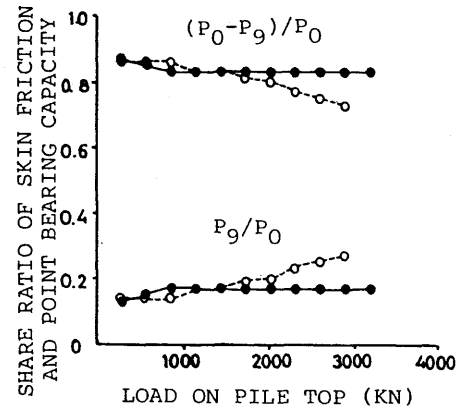


Fig.10 Change of Share Ratio (CASE.2)

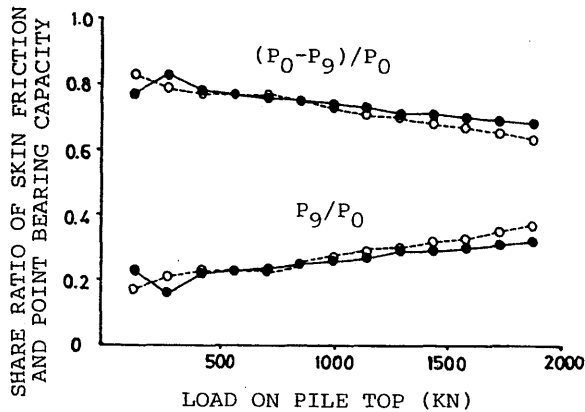


Fig.9 Change of Share Ratio (CASE.1)

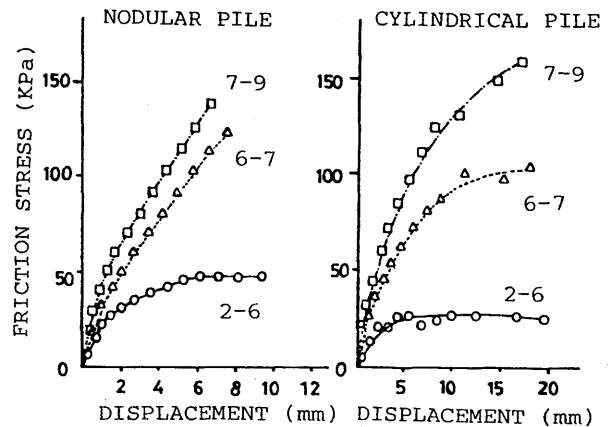


Fig.11 Frictional Stress and Displacement

These figures plot the changes in axial load at each depth in relation to the load acting on the pile head. For the pile head, as the axial load was equal to the applied load, that is on a 45 line, while axial load at each depth became smaller due to the skin friction of the pile. As the difference in the axial load becomes constant when the axial load at each depth is in parallel with this line, the line is considered to indicate a condition where the skin friction yields in the parallel section. It can be assumed from Fig. 8 that the depth at which skin friction yields and becomes constant is up to 5 m (6 sections) from the ground level for the nodular piles and up to 7 m (7 sections) for the cylindrical piles. Furthermore, Fig.9 and 10 show the ratio, expressed in terms of the pile head load, of the point and skin friction resistance which share the load acting on the pile head. Fig.9 indicated that changes in the ratio of share by the cylindrical piles appeared earlier than in the nodular piles when the

pile head load exceed 100 t. A similar trend can be seen in Fig.10. Fig.11 show the relationship between the average frictional stress and the relative displacement of the piles. It is clear from these figures that the frictional stress became larger along with the displacement, but it stopped increasing at a certain displacement level and remained constant. While the frictional stress at shallow depths became constant at displacement of around 5mm, the frictional stress at deep depths was not constant. This tendency corresponds with the variation diagram showing the axial load in Fig.8.

3.2 Results of Horizontal Load Tests

The relationship between horizontal load and deflection is shown in Fig.12 and Fig. 13. In CASE 1, after load was applied in 4 cycles, load was applied until displacement reached about 40 mm. It can be seen

from Fig.12 that the nodular and cylindrical piles have similar relationship between the load-displacement. Although the difference in sectional rigidity between the nodular and cylindrical piles was about 2 times, similar behavior was shown. This may have resulted because the cement milk injected solidified around the nodular piles, and behaved as part of

the piles. In the horizontal alternating load shown in Fig.13, displacement of the cylindrical piles as more alternations were made. This indicated a tendency that is different from Fig.12, and may be due to different loading methods although a clear reason could not be determined.

Fig.14 shows the results of calculating the bending moment distribution of the pile based on the strain gauge installed on the test piles. The coefficient of horizontal subgrade reaction (K value) from load and displacement of the pile top are shown in Fig.15 and Fig.16.

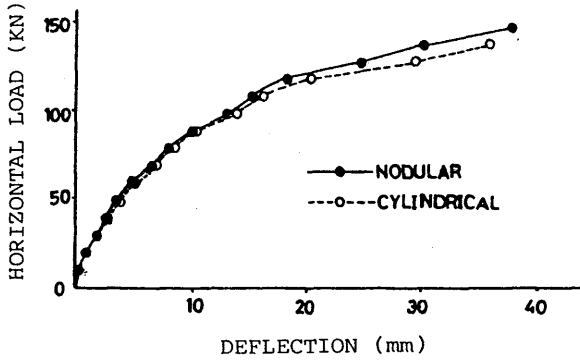
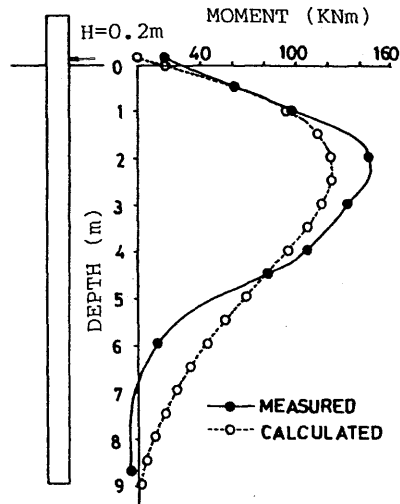


Fig.12 Relationship between Horizontal Load and Deflection (CASE.1)



(a)CYLINDRICAL PILE

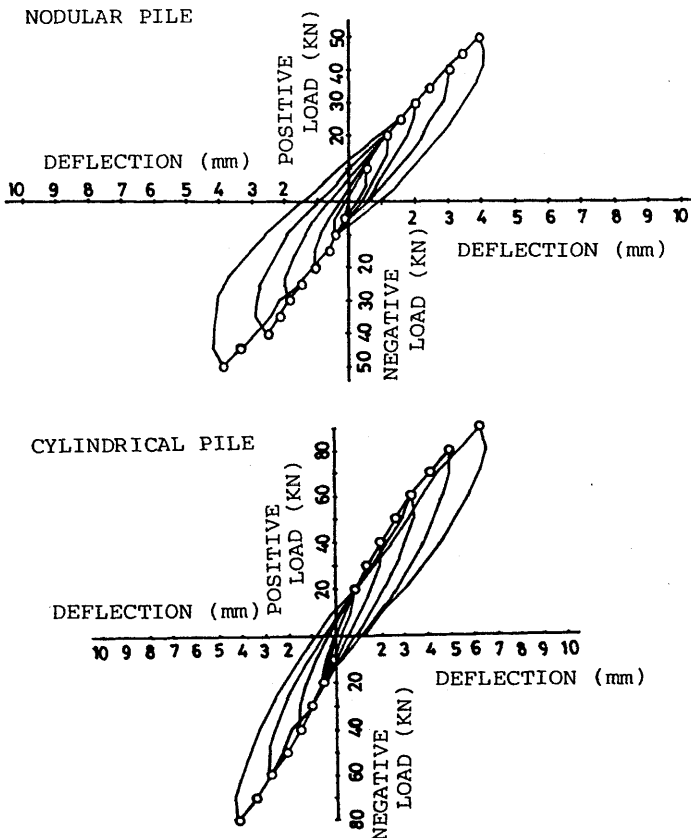
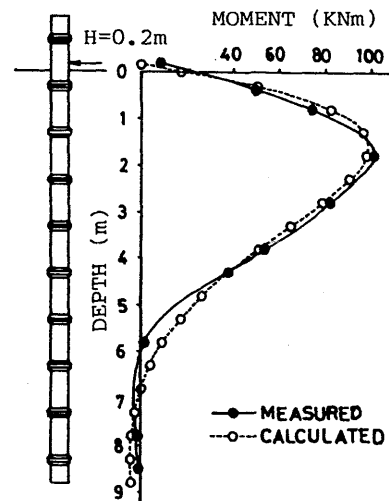


Fig.13 Relationship between Horizontal Load and Deflection (CASE.2)



(b)NODULAR PILE

Fig.14 Bending Moment Distribution (CASE.1)

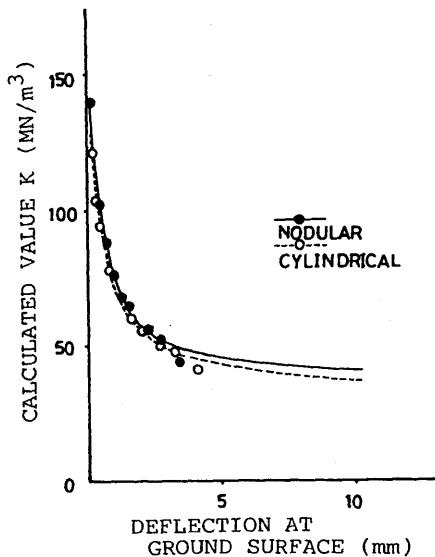


Fig.15 Relationship between K value and Deflection (CASE.1)

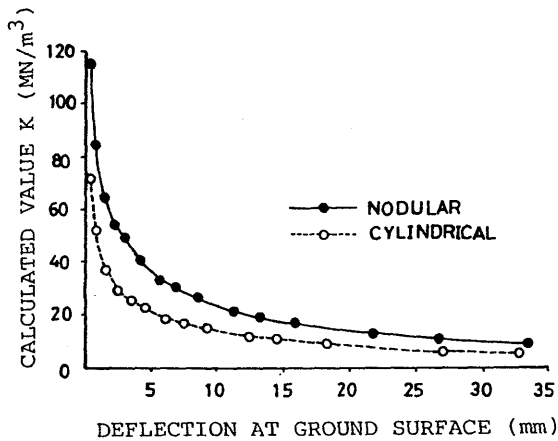


Fig.16 Relationship between K value and Deflection (CASE.2)

Fig.14 also shows the calculation results of the bending moment of the pile using the K value obtained from the tests. According to the Fig.14, the measured depth at which the maximum bending moment was generated in the pile was well agreed with the calculated depth. In the case of the nodular piles, distribution of bending moment in these value corresponded with each other; however, in the case of the cylindrical piles, distribution did not correspond. This may be due to the fact that the maximum bending moment of the cylindrical pile exceeded the cracking/bending moment(=10.5m). The coefficient of horizontal subgrade reaction shown in Fig.15 and 16 became smaller as the displacement increased. In Case 1, the nodular

piles showed a large coefficient subgrade reaction whereas in Case 2, both pile types were almost equal.

4 CONCLUSION

From the tests, the following items became known:

4.1 Inserting a nodular pile resulted in better vertical bearing characteristics compared with that of a cylindrical pile. The ultimate bearing capacity was 1.2-1.5 larger for the nodular piles than the cylindrical piles. This may be because the skin friction of the pile was acting effectively.

4.2 The ratio of point and skin friction resistance was equal during low load degree, for both the nodular and cylindrical piles. As load increased, the skin friction of the cylindrical piles was yielded faster than that of the nodular piles, and it was also found that load on pile head was transmitted to the pile end at an early stage.

4.3 Although the bending rigidity of the piles differed by about twice, both piles showed the same horizontal bearing characteristics; no difference was recognized.

REFERENCES

- Chang, Y.L.: Discussion on "Lateral Pile-Loading Test" by L.B. Feagin, *Trance ASCE*, Vol.102, pp. 272-278, 1937
- Van Der Veen: The Bearing Capacity of a Pile; *Proc. 3rd., ICSMFE*, Vol.2, pp.88-90, 1953
- Ohsugi, F.: Vertical Bearing Capacity of Nodular Piles; *Proc. 17th, JSSMFE*, pp. 2101-2104, 1982